

Muonium spectrum beyond the nonrelativistic limit

Axel Weber

*Instituto de Física y Matemáticas, Universidad Michoacana de San Nicolás de Hidalgo,
Edificio C-3, Ciudad Universitaria, A.P. 2-82, 58040 Morelia, Michoacán, Mexico*

Abstract. A generalization of the Gell-Mann–Low theorem is applied to the antimuon-electron system. The bound state spectrum is extracted numerically. As a result, fine and hyperfine structure are reproduced correctly near the nonrelativistic limit (and for arbitrary masses). We compare the spectrum for the relativistic value $\alpha = 0.3$ with corresponding calculations in light-front quantization.

Keywords: relativistic bound states, muonium

PACS: 11.10.St, 03.65.Ge, 11.10.Ef

More than thirty years have passed since quantum chromodynamics (QCD) has been formulated. Overwhelming evidence has accumulated during this time that QCD gives a complete description of hadronic physics at every energy scale currently accessible to experiment. However, the status of the theory is not at all satisfactory: we are still searching for a deeper understanding of the interaction between quarks and gluons that arises from the QCD Lagrangian beyond the high momentum transfer limit where perturbation theory is applicable. Parts of the physical spectrum that is generated by the theory can be determined through lengthy numerical calculations on space-time lattices which, however, do not provide major insights into the underlying dynamics. Ideally, one would like to have an analytical description of the interaction between quarks and gluons derived from the QCD Lagrangian, typically in the form of an approximation and a systematic procedure to incorporate corrections to the latter. No such description is available to date. Moreover, once it is obtained, we still face the problem of calculating the bound states resulting from this interaction, i.e., the physical hadrons.

The present contribution deals with this second step in connecting the theory in a transparent way with the phenomenology. Without an appropriate description of the fundamental interaction at hand, we consider a simpler theory, namely, quantum electrodynamics (QED), which still has some features in common with QCD. In order to simulate a relativistic situation like the one that prevails in the lighter hadrons, we artificially consider larger coupling constants. E.g., $\alpha = 0.3$ was used before in light-front calculations we will compare with later on. For concreteness, we will consider muonium, a bound state of an antimuon with an electron, although we will allow for an arbitrary antimuon mass. In the special case of equal masses of electron and “antimuon”, the system is similar to positronium if we disregard all (virtual and real) annihilation processes there.

Our approach to relativistic bound states is an application of a generalization of the Gell-Mann–Low theorem [1] to the subspace of Fock space that contains all states of one electron and one antimuon (and no photon). As in the earlier applications of the

same formalism to the Wick-Cutkosky model and Yukawa theory [2, 3], the effective Hamiltonian generated by the generalized Gell-Mann-Low theorem contains the relativistic kinetic energies of the constituents and an effective potential. To lowest order in a perturbative expansion, the matrix elements of the effective potential read, in Coulomb gauge,

$$\begin{aligned}
\langle \mathbf{p}_A, r; \mathbf{p}_B, s | V_{\text{eff}} | \mathbf{p}'_A, r'; \mathbf{p}'_B, s' \rangle &= - \frac{e^2}{\sqrt{2E_{\mathbf{p}_A}^A 2E_{\mathbf{p}_B}^B 2E_{\mathbf{p}'_A}^A 2E_{\mathbf{p}'_B}^B}} \\
&\times \left[\frac{1}{(\mathbf{p}_A - \mathbf{p}'_A)^2} [\bar{u}_A(\mathbf{p}_A, r) \gamma^0 u_A(\mathbf{p}'_A, r')] [\bar{u}_B(\mathbf{p}_B, s) \gamma^0 u_B(\mathbf{p}'_B, s')] \right. \\
&- \frac{1}{2|\mathbf{p}_A - \mathbf{p}'_A|} \left(\frac{1}{E_{\mathbf{p}_A}^A + |\mathbf{p}_A - \mathbf{p}'_A| - E_{\mathbf{p}'_A}^A} + \frac{1}{E_{\mathbf{p}_B}^B + |\mathbf{p}_B - \mathbf{p}'_B| - E_{\mathbf{p}'_B}^B} \right) \\
&\times [\bar{u}_A(\mathbf{p}_A, r) \gamma^j u_A(\mathbf{p}'_A, r')] \left(\sum_{\lambda=1}^2 \varepsilon_i^{(\lambda)}(\mathbf{p}_A - \mathbf{p}'_A) \varepsilon_j^{(\lambda)*}(\mathbf{p}_A - \mathbf{p}'_A) \right) \\
&\left. \times [\bar{u}_B(\mathbf{p}_B, s) \gamma^j u_B(\mathbf{p}'_B, s')] \right] (2\pi)^3 \delta(\mathbf{p}_A + \mathbf{p}_B - \mathbf{p}'_A - \mathbf{p}'_B). \quad (1)
\end{aligned}$$

Here, $|\mathbf{p}_A, r; \mathbf{p}_B, s\rangle$ symbolizes the state of an electron with 3-momentum \mathbf{p}_A and spin orientation r (in a spinor basis yet to be specified) and an antimuon with 3-momentum \mathbf{p}_B and spin orientation s . We use the shorthands $E_{\mathbf{p}_A}^A = (m_A^2 + \mathbf{p}_A^2)^{1/2}$ and $E_{\mathbf{p}_B}^B = (m_B^2 + \mathbf{p}_B^2)^{1/2}$ for the kinetic energies. For convenience, we have introduced the charge-conjugate Dirac spinors $u_B(\mathbf{p}_B, s)$ for the antimuon, while $u_A(\mathbf{p}_A, s)$ represents the electron spinors. The spatially transverse photon polarization vectors $\varepsilon_i^{(\lambda)}(\mathbf{k})$ satisfy the relation $\sum_{\lambda=1}^2 \varepsilon_i^{(\lambda)}(\mathbf{k}) \varepsilon_j^{(\lambda)*}(\mathbf{k}) = \delta_{ij}^{\text{tr}}(\mathbf{k}) = \delta_{ij} - \hat{k}_i \hat{k}_j$ (where $\hat{\mathbf{k}} = \mathbf{k}/|\mathbf{k}|$).

As for the interpretation of the effective potential (1), the second line stems from the instantaneous Coulomb potential, easily identified by the momentum dependence in the denominator (the Fourier transform of the spatial Coulomb potential), and multiplied with the charge densities of the Dirac currents. The following lines are the result of transverse photon exchange, the more complicated denominator indicating a retarded interaction, and the Dirac currents being contracted with the corresponding photon polarization vectors.

The delta function in Eq. (1) shows that total 3-momentum is conserved by the effective interaction, and in the following we will consider the center-of-mass system (c.m.s.) $\mathbf{p}_A + \mathbf{p}_B = \mathbf{p}'_A + \mathbf{p}'_B = 0$. In order to simplify the diagonalization of the effective Hamiltonian, we express the Dirac spinors in terms of Pauli spinors (using the Dirac-Pauli representation) to find for the effective Schrödinger equation in the c.m.s.,

$$\left(\sqrt{m_A^2 + \mathbf{p}^2} + \sqrt{m_B^2 + \mathbf{p}^2} \right) \phi(\mathbf{p}) - e^2 \int \frac{d^3 p'}{(2\pi)^3} \sqrt{\frac{E_{\mathbf{p}}^A + m_A}{2E_{\mathbf{p}}^A} \frac{E_{\mathbf{p}}^B + m_B}{2E_{\mathbf{p}}^B} \frac{E_{\mathbf{p}'}^A + m_A}{2E_{\mathbf{p}'}^A} \frac{E_{\mathbf{p}'}^B + m_B}{2E_{\mathbf{p}'}^B}}$$

$$\begin{aligned}
& \times \left[\frac{1}{(\mathbf{p} - \mathbf{p}')^2} \left(1 + \frac{\mathbf{p} \cdot \boldsymbol{\sigma}_A}{E_{\mathbf{p}}^A + m_A} \frac{\mathbf{p}' \cdot \boldsymbol{\sigma}_A}{E_{\mathbf{p}'}^A + m_A} \right) \left(1 + \frac{\mathbf{p} \cdot \boldsymbol{\sigma}_B}{E_{\mathbf{p}}^B + m_B} \frac{\mathbf{p}' \cdot \boldsymbol{\sigma}_B}{E_{\mathbf{p}'}^B + m_B} \right) \right. \\
& + \frac{1}{2|\mathbf{p} - \mathbf{p}'|} \left(\frac{1}{E_{\mathbf{p}}^A + |\mathbf{p} - \mathbf{p}'| - E_{\mathbf{p}'}^A} + \frac{1}{E_{\mathbf{p}}^B + |\mathbf{p} - \mathbf{p}'| - E_{\mathbf{p}'}^B} \right) \left(\frac{(\mathbf{p} \cdot \boldsymbol{\sigma}_A) \sigma_A^i}{E_{\mathbf{p}}^A + m_A} + \frac{\sigma_A^i (\mathbf{p}' \cdot \boldsymbol{\sigma}_A)}{E_{\mathbf{p}'}^A + m_A} \right) \\
& \left. \times \delta_{ij}^{\text{tr}}(\mathbf{p} - \mathbf{p}') \left(\frac{(\mathbf{p} \cdot \boldsymbol{\sigma}_B) \sigma_B^j}{E_{\mathbf{p}}^B + m_B} + \frac{\sigma_B^j (\mathbf{p}' \cdot \boldsymbol{\sigma}_B)}{E_{\mathbf{p}'}^B + m_B} \right) \right] \phi(\mathbf{p}') = E' \phi(\mathbf{p}). \quad (2)
\end{aligned}$$

Here, $\mathbf{p} = \mathbf{p}_A = -\mathbf{p}_B$, the spinorial wave function $\phi(\mathbf{p})$ is defined as $\phi(\mathbf{p}_A)(2\pi)^3 \delta(\mathbf{p}_A + \mathbf{p}_B) = \sum_{r,s} \langle \mathbf{p}_A, r; \mathbf{p}_B, s | \phi \rangle [\chi_r \otimes \chi_s]$, and $\boldsymbol{\sigma}_A$ ($\boldsymbol{\sigma}_B$) is understood to act on the Pauli spinor χ_r (χ_s) only. E' is the difference between the energy of the bound state and the vacuum energy. Of the full state $|\phi\rangle$ in Fock space (with zero total momentum), only its projection to one-electron–one-antimuon states $|\mathbf{p}_A, r; \mathbf{p}_B, s\rangle$ appears. The effect of its components in other Fock space sectors is taken care of implicitly by the effective potential.

In order to solve the Schrödinger equation (2), we take into account its rotational symmetry. Eigenstates of total angular momentum J can be constructed as usual by adding relative orbital angular momentum L and total spin S . For convenience, we will label the eigenstates by the “relative parity” π' defined through $(-1)^L = \pi'(-1)^J$. Since $S = 0, 1$, for given J the sector $\pi' = +1$ contains the states with $L = J$ and $S = 0$ or $S = 1$, while for $\pi' = -1$ we can have $L = J - 1$ or $L = J + 1$, with $S = 1$ in both cases. In any sector $J^{\pi'}$, the two different possible (LS) -states will mix, except in the following cases: (i) for $J = 0$, $J^{\pi'} = 0^+$ is only realized by $(L = 0, S = 0)$, and 0^- only by $(L = 1, S = 1)$; (ii) in the case of equal masses, the Hamiltonian acquires an additional symmetry under the exchange of particles A and B ; as a result, S becomes a good quantum number and there is no mixing in the $(\pi' = +1)$ -sector; (iii) in the one-body limit where one of the masses goes to infinity, the spin of the heavy particle decouples from the dynamics; as a result, every two states are degenerate in this limit and L becomes a good quantum number [no mixing in the $(\pi' = -1)$ -sector].

After explicitly carrying out the contractions of the spatial indices in the transverse photon exchange part, the formulae derived before for the application to Yukawa theory [3] can be used to determine the result of the application of the terms containing the Pauli matrices in Eq. (2) to the total angular momentum eigenstates. On the other hand, the application of the factors containing $|\mathbf{p} - \mathbf{p}'|$ on orbital angular momentum eigenstates proceeds through the partial wave decomposition of the former. The partial wave decomposition of the (Fourier transformed) Coulomb potential is well-known, the one for the δ_{ij} -part of the transverse photon exchange has been calculated in Ref. [3]. The partial waves of the $\hat{k}_i \hat{k}_j$ -part of the transverse photon exchange are given by

$$\begin{aligned}
b_L(p, p') &= \frac{2L+1}{2} \int_{-1}^1 d \cos \theta P_L(\cos \theta) \\
& \times \frac{1}{(\mathbf{p} - \mathbf{p}')^2} \frac{1}{2|\mathbf{p} - \mathbf{p}'|} \left(\frac{1}{E_{\mathbf{p}}^A + |\mathbf{p} - \mathbf{p}'| - E_{\mathbf{p}'}^A} + \frac{1}{E_{\mathbf{p}}^B + |\mathbf{p} - \mathbf{p}'| - E_{\mathbf{p}'}^B} \right). \quad (3)
\end{aligned}$$

This integral diverges like $(p - p')^{-2}$ for $p' \rightarrow p$ which would lead to a divergence in the p' -integral. These divergences, of course, are spurious and cancel in pairs. However, for the numerical calculation, we have to extract the divergent parts and perform the cancellations analytically. Fortunately, the extraction of the divergencies is simple: they occur at $\cos \theta = 1$, and since $P_L(1) = 1$, we can define “reduced” Legendre polynomials $P_L^R(\cos \theta)$ through

$$P_L(\cos \theta) - 1 = (\cos \theta - 1) P_L^R(\cos \theta). \quad (4)$$

Separating the one on the l.h.s. of Eq. (4) under the integrals (3), the remainder of the integrals is logarithmically divergent for $p' \rightarrow p$ (as are the other partial waves), and the following p' -integration is convergent. The divergent parts in Eq. (3) originating from the one in Eq. (4) can be analytically cancelled in pairs, leaving a finite contribution.

Putting everything together, the potential term in the Schrödinger equation (2) reduces to a one-dimensional integral over p' when applied to the total angular momentum eigenstates. For every sector $J^{\pi'}$, two such equations are coupled (with the exceptions mentioned above). The explicit expressions for the integral kernels (diagonal and off-diagonal because of the coupling) are quite lengthy and cannot be reproduced here due to lack of space.

The (coupled) one-dimensional integral equations can be solved by expanding the wave function in an appropriate orthonormal basis. After reducing the basis to a finite number of elements (40 in our calculations), the integral equations are approximately replaced by finite matrix equations. The matrix elements are two-dimensional integrals which are calculated numerically (we use a two-dimensional grid of 400×800 points). Finally, the matrices are numerically diagonalized to give the (approximate) eigenvalues and eigenstates of Eq. (2). The results for the lowest energy eigenvalues are plotted in Figs. 1 and 2 for equal constituent masses and fine structure constants $\alpha \leq 0.45$. The binding energies are normalized to $\mu\alpha^2$, μ being the reduced mass, so that the comparison with the nonrelativistic energy eigenvalues $\mu\alpha^2/2n^2$ is immediate.

We find that for values $\alpha < 0.1$, the energy levels are dominated by the nonrelativistic values plus the leading relativistic corrections (the leading-order fine and hyperfine structure) of order $\mu\alpha^4$, both in our numerical results and in the perturbative calculations of bound-state QED. In this region of small coupling constants, the numerical results are in good agreement with the perturbative calculations, apparently only limited by the numerical precision. For larger values $\alpha > 0.1$, higher perturbative orders become important and our numerical results deviate in some cases strongly from the lowest-order perturbative predictions.

In Table 1 we compare our results for $\alpha = 0.3$ with two different calculations in light front quantization [4, 5] (we use the data for the Gaussian similarity function in the latter paper). In the table, we label the states by the nonrelativistic notation $n^{2S+1}L_J$ and also indicate the corresponding sectors $J^{\pi'}$. There is a clear tendency in our results towards more negative energies, i.e., stronger binding, compared to $\mathcal{O}(\mu\alpha^4)$ -perturbation theory. The ordering of the different levels, however, is the same as in perturbation theory. We can also see that the difference to perturbation theory in the direction of stronger binding is systematically larger for S -states than for P -states, and also larger for $(J = 0)$ -states than for $(J = 1)$ -states, and smallest for the $(J = 2)$ -state. For the light-front results, this latter tendency is inverted; the S_0 -states have even higher energies than in perturbation

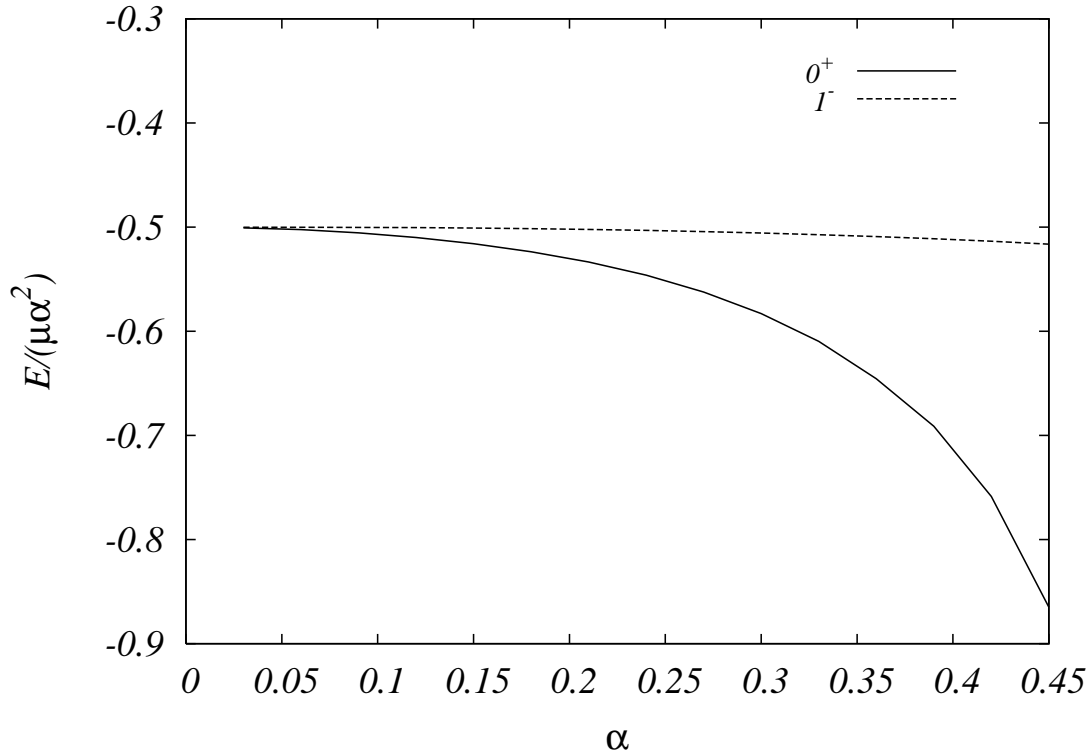


FIGURE 1. The binding energy $E = E' - m_A - m_B$ as a function of the fine structure constant $\alpha = e^2/4\pi$ for the case of equal masses $m_A = m_B$. E is normalized to $\mu\alpha^2$ where μ is the reduced mass ($\mu = m_A/2$ in the present case). Plotted are the lowest energy levels for $J^{\pi'} = 0^+$ and 1^- corresponding to the nonrelativistic principal quantum number $n = 1$.

TABLE 1. Binding energies $E/\mu\alpha^2$ for equal masses from perturbation theory to $\mathcal{O}(\mu\alpha^4)$, from our numerical results, and from Refs. [4] and [5]

state	perturbation theory	our results	Ref. [4]	Ref. [5]
$1^1S_0(0^+)$	-0.559	-0.583	-0.525	-0.551
$1^3S_1(1^-)$	-0.499	-0.506	-0.501	-0.525
$2^1S_0(0^+)$	-0.1343	-0.1373	-0.1301	-0.1332
$2^3P_0(0^-)$	-0.1306	-0.1315	-0.1335	-0.1369
$2^3P_1(1^+)$	-0.1278	-0.1279	-0.1298	-0.1327
$2^3S_1(1^-)$	-0.1268	-0.1277	-0.1269	-0.1298
$2^1P_1(1^+)$	-0.1268	-0.1269	-0.1290	-0.1315
$2^3P_2(2^-)$	-0.1255	-0.1255	-0.1277	-0.1302

theory. Both light-front calculations are qualitatively similar, only that the binding is stronger throughout in the similarity transform approach of Ref. [5]. In conclusion, we find very different results with the two different methods for relativistic bound state calculations (in the approximations presently considered). We should remark, however,

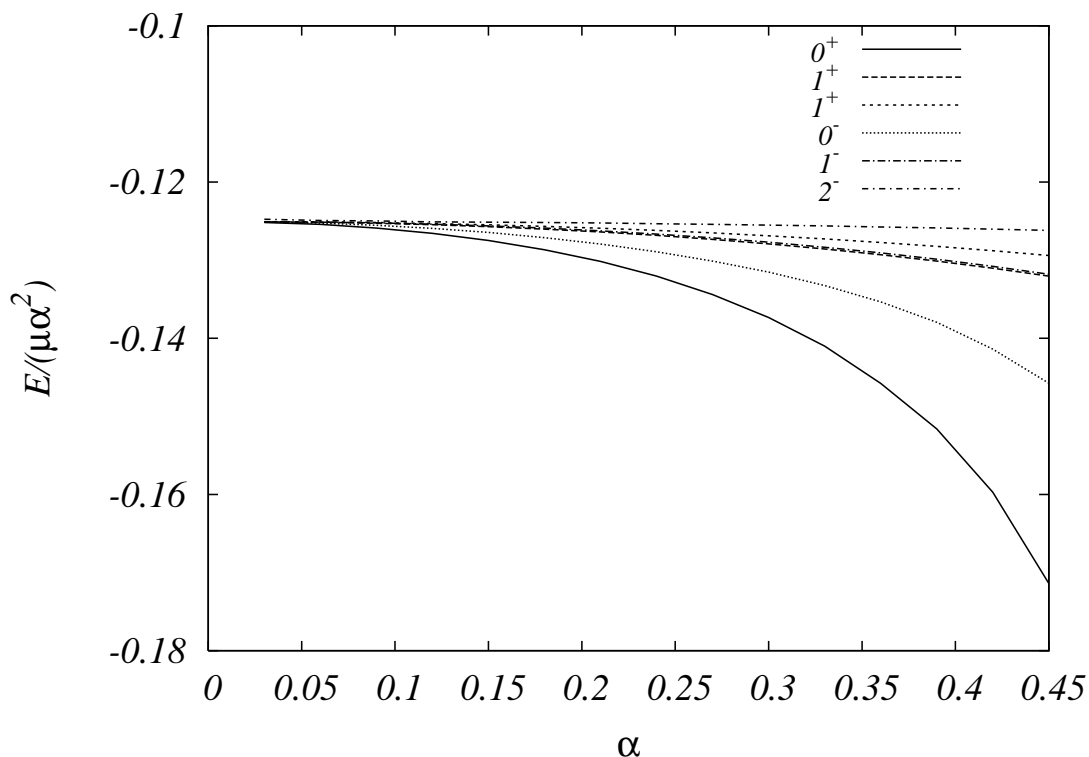


FIGURE 2. As Fig. 1, but for the energy levels corresponding to the nonrelativistic principal quantum number $n = 2$.

that there is an unphysical logarithmic UV cutoff dependence in the light-front results (for the cited values, the cutoff has been set equal to the constituent masses).

ACKNOWLEDGMENTS

Support by Conacyt grant 46513-F and CIC-UMSNH is gratefully acknowledged. I thank my collaborator Juan Carlos López Vieyra for performing the numerical calculations and elaborating the graphics.

REFERENCES

1. A. Weber, in *Particles and Fields — Seventh Mexican Workshop*, edited by A. Ayala, G. Contreras, and G. Herrera, AIP Conf. Proc. No. 531, AIP, New York, 2000, pp. 305–309, preprint hep-th/9911198.
2. A. Weber, and N. E. Ligterink, *Phys. Rev. D* **65**, 025009 (2002).
3. A. Weber, and N. E. Ligterink, “Bound states in Yukawa theory”, preprint hep-ph/0506123.
4. U. Trittman, and H.-C. Pauli, “Quantum electrodynamics at strong couplings”, preprint hep-th/9704215.
5. E. L. Gubankova, H.-C. Pauli, F. J. Wegner, and G. Papp, “Light-cone Hamiltonian flow for positronium”, preprint hep-th/9809143.